Atmos. Chem. Phys. Discuss., 15, 15319–15354, 2015
www.atmos-chem-phys-discuss.net/15/15319/2015/
doi:10.5194/acpd-15-15319-2015

Atmospheric Chemistry and Physics
Discussions
Open Access

Spatial and temporal variations of the concentrations of PM_{10}, $PM_{2.5}$ and PM_1 in China

Y. Q. Wang[1], X. Y. Zhang[1], J. Y. Sun[1], X. C. Zhang[2], H. Z. Che[1], and Y. Li[1]

[1]Laboratory of Atmospheric Chemistry, Chinese Academy of Meteorological Sciences, Beijing, China
[2]Meteorological Observation Center, Beijing, China

Received: 26 March 2015 – Accepted: 25 April 2015 – Published: 8 June 2015

Correspondence to: Y. Q. Wang (yaqiang.wang@gmail.com)

Published by Copernicus Publications on behalf of the European Geosciences Union.

Spatial and temporal variations of the concentrations of PM_{10}, $PM_{2.5}$ and PM_1 in China

Y. Q. Wang et al.

Abstract

Concentrations of PM_{10}, $PM_{2.5}$ and PM_1 were monitored at 24 stations of CAWNET (China Atmosphere Watch Network) from 2006 to 2014 using GRIMM 180 dust monitors. The highest particulate matter (PM) concentrations were observed at the stations of Xian, Zhengzhou and Gucheng, in Guanzhong and the Hua Bei Plain (HBP). The second highest PM concentrations were observed in northeast China, followed by southern China. According to the latest air quality standards of China, 14 stations reached the PM_{10} standard and only 7 stations, mainly rural and remote stations, reached the $PM_{2.5}$ standard. The $PM_{2.5}$ and PM_{10} ratios showed a clear increasing trend from northern to southern China, because of the substantial contribution of coarse mineral aerosol in northern China. The PM_1 and $PM_{2.5}$ ratios were higher than 80 % at most stations. PM concentrations tended to be highest in winter and lowest in summer at most stations, and mineral dust impacts influenced the results in spring. A decreasing interannual trend was observed in the HBP and southern China from 2006 to 2014, but an increasing trend occurred at some stations in northeast China. Also diurnal variations of PM concentrations and meteorological factors effects were investigated.

1 Introduction

Tropospheric aerosols are important because of their strong influence on the climate system through both direct and indirect effects. These include the direct effect of scattering and absorbing radiant energy and the indirect effect of modifying the microphysical properties of clouds, and hence their radiative properties and lifetime (Haywood and Boucher, 2000). They also attract attention because of their effects on visibility impairment (Watson, 2002) and human health (Delfino et al., 2005; Pope III and Dockery, 2006). Therefore, the spatial and temporal variation of aerosols is essential to

ACPD
15, 15319–15354, 2015

understand, but remains a complex subject because of the relatively short lifetime and complexity of aerosol physical and chemical properties (Ramanathan et al., 2001).

Particle size is considered a key parameter to define the impact of particulate matter (PM) on human health; fine PM ($PM_{2.5}$ and PM_1) poses a greater health risk than coarse PM (PM_{10}) (Oberdörster et al., 2005). There have been numerous network-based observation studies of the $PM_{2.5}$ concentration and chemical composition in North America and Europe. For example, based on a dataset across 19 Canadian sites, most of the $PM_{2.5}$ concentrations were found to be below 26 $\mu g\,m^{-3}$, and $PM_{2.5}$ accounted for 49 % of the measured PM_{10} (Brook et al., 1997). $PM_{2.5}$ and PM_{10} particulate concentrations measured at 42 sites in the Interagency Monitoring of Protected Visual Environments (IMPROVE) network over the 1993 seasonal year (March 1993 to February 1994) showed the $PM_{2.5}$ concentration had a large gradient from west to east in the US, averaging 3 $\mu g\,m^{-3}$ in most of the west compared with 13 $\mu g\,m^{-3}$ in the Appalachian region (Eldred et al., 1997). Another study based on 143 sites of IMPROVE in the year 2001 showed that sulfates, carbon and crustal material were responsible for most of the measured $PM_{2.5}$ at the majority of sites in the US (Malm et al., 2004). The temporal variation and spatial distribution of $PM_{2.5}$ concentrations have also been reported in Switzerland (Gehrig and Buchmann, 2003), Austria (Gomiscek et al., 2004) and six central and eastern European countries (Houthuijs et al., 2001).

As a country with a rapidly developing economy, China has suffered from a serious air pollution problem in recent years due to substantial increases in energy consumption and other related production of large amounts of aerosols and precursor gas emissions (Zhang et al., 2009). The spatial distribution and interannual variation of PM_{10} concentrations was studied using a dataset accumulated from 86 Chinese cites (Qu et al., 2010). The chemical compositions of PM_{10} samples were investigated at 16 sites over China, and the result indicated a dominant scattering feature of aerosols in China (Zhang et al., 2012). Existing studies of network $PM_{2.5}$ observations have been limited to certain seasons in a single year (Cao et al., 2012), and most other research has focused on one or more of the largest cities (He et al., 2001; Wang et al., 2002, 2006; Wei et al., 1999; Yao et al., 2002; Zhao et al., 2009; Zheng et al., 2005).

The heavy haze problem encourages the Chinese government to pay more attention to $PM_{2.5}$ monitoring and air quality standards. The Ministry of Environmental Protection of China issued new ambient air quality standards in 2012, among which the $PM_{2.5}$ concentration was the first to be included. Subsequently, construction of a national environmental $PM_{2.5}$ monitoring station network began in 2013.

In this paper, we firstly present a long-term PM_{10}, $PM_{2.5}$ and PM_1 monitoring dataset from 2006 to 2014, based on 24 stations of CAWNET (China Atmosphere Watch Network), operated by the China Meteorological Administration (CMA). The spatial pattern of average PM concentration levels and the relationships among them are reported. In addition, their seasonal, interannual and diurnal variations and meteorological factors effects are presented.

2 The near real-time PM dataset

The PM_{10}, $PM_{2.5}$ and PM_1 concentrations were monitored at 24 stations of CAWNET from 2006 to 2014 using GRIMM dust monitor EDM 180 instruments with 31 different size channels at a flow rate of 1.2 L min^{-1}. The instrument was designed to measure particle size distribution and particulate mass, based on a light scattering measurement of individual particles in the sampled air. GRIMM developed protocols were used to convert the measured size number distribution to a mass concentration consistent with U.S. Environmental Protection Agency protocols for measuring particulate matter based on aerodynamic diameter. A Nafion dryer was equipped at the inlet to exclude fine particulate water, but the nonvolatile and semi-volatile components are included in the measurement result (Grimm and Eatough, 2009). The GRIMM instruments were calibrated annually using a calibration tower that permitted powder injection (on demand) of aerosol particles in a wide size range of 0.2–30 µm. The operation was fully computer controlled and permitted access to one to three spectrometers in comparison

ACPD
15, 15319–15354, 2015

to one reference "mother unit". The 5 min averaged PM_{10}, $PM_{2.5}$ and PM_1 concentrations were recorded at each station and transported to the CMA information center hourly in near real-time.

The PM concentration data results from GRIMM instrument were compared to the results from tapered element oscillating microbalances (TEOM) instrument in some studies (Grimm and Eatough, 2009; Hansen et al., 2010). The instruments were in good agreement, e.g. linear regression of the Grimm vs. the FDMS TEOM data in Rubidoux yielded a slope of 1.10 ± 0.05 with an intercept of $-3.9 \pm 4.2\,\mu g\,m^{-3}$, and the uncertainty was 9.9 % (Grimm and Eatough, 2009).

The 24 PM observation stations are described in Table 1, and a map of their distribution is given in Fig. 1. Most stations were located in East China, an area of high population density and fast economic development; therefore, PM emitted from human activities was mainly recorded. The stations were classified as urban/suburban, rural and remote stations according to their location. Unlike rural stations, remote stations were located in areas far away from regions of strong anthropogenic emissions, and thus natural emissions and long-range transport of anthropogenic air pollution were the main sources of PM at these stations.

3 Results and discussion

3.1 Average PM_{10}, $PM_{2.5}$ and PM_1 levels in China

The averaged PM concentration values are presented in Table 2. A distribution bar chart map of the averaged PM concentrations is presented in Fig. 2. The highest PM_{10}, $PM_{2.5}$ and PM_1 concentrations were observed at the stations of Xian (135.4, 93.6 and $77.0\,\mu g\,m^{-3}$, respectively), Zhengzhou (131.7, 84.8 and $71.0\,\mu g\,m^{-3}$, respectively) and Gucheng (127.8, 89.7 and $79.4\,\mu g\,m^{-3}$, respectively), which are located in the most polluted areas of the Hua Bei Plain (HBP) and Guanzhong Plain. Although Gucheng is a suburban site, it is located in the rapidly urbanizing area around Beijing, and is

ACPD
15, 15319–15354, 2015

therefore subject to associated large quantities of air pollution emissions. These areas were also identified by Zhang et al. (2012) as Region II with similar visibility change and large visibility loss in the past 40 years. The stations all recorded very high coarse and fine PM concentrations, implying high emissions of both primary emitted mineral particles and secondary formatted particles in these areas. Qingdao is a coastal city with relatively low PM concentrations compared with inland cities in the HBP.

The PM concentrations were also high in northeast China, which is an established industrial base area. The ensemble average values of the five urban stations of Ansan, Shenyang, Benxi, Fushun and Shiping were 88.8, 58.4 and 49.8 $\mu g\,m^{-3}$, for PM_{10}, $PM_{2.5}$ and PM_1 respectively. Dandong is a rural station with relatively low PM concentrations.

The similarity among the PM values for Chifeng, Erlianhaote and Yulin is due to their location, far from regions of intensive economic development, and is also strongly affected by sand and dust storms, given the stations are located adjacent to dust source areas. Thus, the average PM_{10} concentrations were much higher than the $PM_{2.5}$ and PM_1 concentrations at these sites. For example, the average PM concentrations were 88.0, 42.4 and 32.6 $\mu g\,m^{-3}$ at Chifeng, which is surrounded by Horqin Sandy Land and Onqin Daga Sandy Land.

Chengdu, the capital of Sichuan Province, is located in the Sichuan Basin, which is also a highly polluted area with high aerosol optical depth and low visibility (Li et al., 2003; Luo et al., 2001; Zhang et al., 2012), due to the poor dispersion conditions and heavy local industrial emissions. The average PM_{10}, $PM_{2.5}$ and PM_1 concentrations were 78.0, 59.5 and 52.7 $\mu g\,m^{-3}$, respectively.

There are three stations in the South China area: Panyu, located in Guangzhou City, the capital of Guangdong Province, which is the center of the Pearl River Delta region; Nanning, the capital of Guangxi Province; and Guilin, a famous tourist city, also located in Guangxi Province. The ensemble average PM concentrations of the three sites were 55.8, 43.1 and 38.8 $\mu g\,m^{-3}$ for PM_{10}, $PM_{2.5}$ and PM_1, respectively.

ACPD
15, 15319–15354, 2015

Significant visibility loss and relatively high PM_{10} concentrations have been observed over the middle and lower reaches of the Yangtze River after the 1980s due to the rapid economic development in the region (Qu et al., 2010; Zhang et al., 2012). Although there was no urban site available in this study to characterize the high PM concentrations in this region, the background conditions and temporal variance could be determined from the rural site data. Dongtan, near Shanghai City, is located on Chongming Island with low PM concentrations (31.9, 27.4 and 24.8 $\mu g\,m^{-3}$ for PM_{10}, $PM_{2.5}$ and PM_1, respectively) due to the substantial influence of clean sea air mass. The ensemble average PM concentrations of Lushan, Changde and Jinsha were 44.3, 37.2 and 33.6 $\mu g\,m^{-3}$ for PM_{10}, $PM_{2.5}$ and PM_1, respectively.

Lhasa, the capital of Tibet Autonomous Region, is located in the center of the Tibetan Plateau at a very high altitude of 3663 m. The $PM_{2.5}$ and PM_1 concentrations in Lhasa were low, with average values of 14.0 and 9.6 $\mu g\,m^{-3}$, respectively, because of its relatively small population and few industrial emissions. However, the average PM_{10} concentration was 37.7 $\mu g\,m^{-3}$, mainly due to the high amounts of fugitive dust from dry and bare land and the impacts of regional dust storm events (Chen et al., 2013). As a result, minerals represent the major component of aerosol samples in this area (Zhang et al., 2012).

The lowest PM concentration values were observed in the two remote sites of Akadala and Shangri-La. The lower altitude and stronger contribution of soil dust at Akadala (Qu et al., 2009), located in a dry region, leads to higher PM concentrations than at the Shangri-La site.

According to the latest air quality standards of China (annual averaged PM_{10} and $PM_{2.5}$ concentrations of 70 and 35 $\mu g\,m^{-3}$), 14 stations reached the PM_{10} standard and only 7 stations, mainly rural and remote stations, reached the $PM_{2.5}$ standard. The ratio of substandard (daily averaged PM_{10} or $PM_{2.5}$ concentrations that exceed the standard values) days to total observation days at each station was calculated using the standard daily averaged PM_{10} and $PM_{2.5}$ concentrations of 150 and 75 $\mu g\,m^{-3}$ (Table 2). Substandard days of PM_{10} and $PM_{2.5}$ represented more than 30 and 50 % of

ACPD
15, 15319–15354, 2015

the total period at the three most polluted sites (Xian, Zhengzhou and Gucheng). The $PM_{2.5}$ substandard days ratios at five other stations (Chengdu, Anshan, Shenyang, Benxi and Siping) were also larger than 20 %.

Average PM_{10}, $PM_{2.5}$ and PM_1 concentrations at urban/suburban stations in this study were 83.6, 56.3 and 48.3 $\mu g\,m^{-3}$, respectively. The values were 54.8, 36.3 and 30.8 $\mu g\,m^{-3}$ at rural stations, and 11.9, 7.5 and 6.1 $\mu g\,m^{-3}$ at remote stations. They are much higher than the results from other countries. The PM concentration data observed in Canada between 1984 to 1993 showed the average $PM_{2.5}$ concentrations were 14.1 and 10.7 $\mu g\,m^{-3}$ at urban and rural stations respectively (Brook et al., 1997). The average $PM_{2.5}$ values were 3 to 13 $\mu g\,m^{-3}$ from west to east US observed from IMPROVE network (most stations were located in rural areas) in 1993 (Eldred et al., 1997). The observation in Swiss from 1998 to 2001 showed the average PM_{10} and $PM_{2.5}$ concentrations at urban/suburban stations were 27.7 and 20.1 $\mu g\,m^{-3}$, respectively (Gehrig and Buchmann, 2003). Annual means of mass concentrations of PM_{10}, $PM_{2.5}$ and PM_1 were in the order of 28, 20 and 16 $\mu g\,m^{-3}$ at the urban sites and a little bit lower at the rural site in Austria in 1998 (Gomiscek et al., 2004). With the rapid urbanization and corresponding increase in the traffic and energy consumption, the ambient concentrations of fine particulate are also high in India. For example, the measurement at New Delhi during the August to December 2007 showed the concentrations of PM_{10}, $PM_{2.5}$ and PM_1 were ranged from 20 to 180 $\mu g\,m^{-3}$ during the monsoon and from 100 to 500 $\mu g\,m^{-3}$ during the winter (Tiwari et al., 2012).

3.2 Relationships between PM_{10}, $PM_{2.5}$ and PM_1 concentrations

The squared correlation coefficient (R^2) values of the linear fit between PM_{10} and $PM_{2.5}$ and between PM_1 and $PM_{2.5}$ are given in Table 2. Higher values indicate that two PM size bins may have more identical-source characteristics. At most stations, the R^2 values between PM_1 and $PM_{2.5}$ were higher than the values between $PM_{2.5}$ and PM_{10}, because PM_1 and $PM_{2.5}$ both belong to fine particle size bins, which are normally

ACPD
15, 15319–15354, 2015

emitted from the same sources. For example, the R^2 values were 0.7857 between $PM_{2.5}$ and PM_{10}, and 0.9689 between PM_1 and $PM_{2.5}$, at Gucheng (Fig. 3). Correlation coefficient analysis is sensitive to outliers, and thus sand storm events may impact the result considerably, due to abnormally high concentration values. There were four strong dust storm event days at Akdala in 2012, on 21 April and 22, and 9 May and 20, which resulted in the four outlier points shown in Fig. 4a, and the low R^2 value of 0.5346 between PM_1 and $PM_{2.5}$. The value increased to 0.9406 when the four outlier points were removed (Fig. 4b). Similar results were also observed at Yulin and Erlianhaote around dust storm source regions (Table 2).

The average values of the daily $PM_{2.5}/PM_{10}$ and $PM_1/PM_{2.5}$ ratios are listed in Table 2. The spatial distribution map of the average $PM_{2.5}/PM_{10}$ ratios (Fig. 5) shows lower ratio values in northern China, influenced by Asian sand and dust storms (Wang et al., 2008; Zhang et al., 2003). The values were also influenced by fugitive dust due to the low precipitation amounts in northern China, especially at Lhasa, Erlanhaote, Yulin and Chifeng, with ratio values of less than 0.6. The ratio values at the stations in northeast China were between 0.6 and 0.7, except at Dandong where the value was 0.71. The values were also low at Zhengzhou and Akdala, at 0.68 and 0.67, respectively. The highest ratio value was 0.9 at Dongtan, and the other stations with ratio values higher than 0.8 were Chengdu, Changde, Guilin, Jinsha and Lushan. The values were between 0.7 and 0.8 at other stations. The $PM_1/PM_{2.5}$ ratios showed a similar spatial distribution, but the values were higher than $PM_{2.5}/PM_{10}$. The lowest ratio value of 0.6 was also observed at Lhasa, and the values at most stations in southern China were greater than or equal to 0.9.

3.3 Seasonal variations

The seasonal variations of PM_{10} concentrations (Fig. 6a) show that winter and spring were the most polluted seasons at all sites except Lushan, where the highest value was observed in autumn. This result is consistent with a previous study of PM_{10} variation across China from 2000 to 2006 (Qu et al., 2010). The higher winter concentrations were caused by higher emissions during the cold season from heating, and more stagnant weather conditions with a lower planetary boundary layer. The opposite conditions and more precipitation due to the summer monsoon resulted in the lowest PM_{10} concentration values in summer. Spring is the dust storm season in East Asia (Qian et al., 2004; Wang et al., 2008; Zhou and Zhang, 2003), which leads to high PM_{10} concentrations in dust source regions and downwind areas in northern China. For example, the PM_{10} concentrations in spring were much higher than other seasons at the dust source sites of Yulin and Erlianhaote.

For $PM_{2.5}$, winter was still the most polluted season at most sites, while the contribution of spring decreased substantially in northern China (Fig. 6b). This trend can be further observed from the PM_1 distribution (Fig. 6c); hence, the average PM_1 concentration of spring was lowest at Yulin, Xian, Zhengzhou, Gucheng and Benxi. The seasonal variation patterns were very similar for PM_{10}, $PM_{2.5}$ and PM_1 at the sites in southern China.

A spatial distribution map of the seasonal average $PM_{2.5}/PM_{10}$ ratios is given in Fig. 6d. For the reasons given above, lower $PM_{2.5}/PM_{10}$ ratios were observed in spring at the northern China sites, while the seasonal variation was not significant at the southern China sites.

3.4 Interannual variations

The interannual variations of $PM_{2.5}$ at various stations are presented in Fig. 7. Significant decreasing trends were observed at the HBP stations of Zhengzhou and Gucheng (Fig. 7a). The annual averaged $PM_{2.5}$ concentrations decreased from 123.4 to 65.2 $\mu g\,m^{-3}$ at Zhengzhou, and from 101.0 to 69.1 $\mu g\,m^{-3}$ at Gucheng, during 2006–2014. At Zhengzhou, the lowest value of 63.7 $\mu g\,m^{-3}$ occurred in 2012, and this level was maintained in subsequent years; however, at Gucheng, the value increased suddenly in 2012 to 95.1 $\mu g\,m^{-3}$ and then declined rapidly during 2013 and 2014. At Xian, the annual averaged $PM_{2.5}$ concentrations decreased from 2006 to 2009, increased until 2011, and then decreased again until 2014 (Fig. 7a).

For the stations in northeast China, a significant increasing trend of $PM_{2.5}$ concentrations was observed at Shenyang and Benxi from 2006 to 2013, followed by a decrease in 2014 (Fig. 7b). The peak value at Shenyang was especially high in 2013 at 123.1 $\mu g\,m^{-3}$, while the values were less than 60 $\mu g\,m^{-3}$ in the other years. The highest values were observed in 2009 at Anshan and Dandong, but the lowest value was in 2014 at Anshan and 2010 at Dandong. A general decreasing trend was observed at Siping, with a few fluctuations. At Fushun, the value decreased from 2006 to 2011 and then increased to 2013, followed by a slight decrease in 2014.

For the stations along the middle and lower reaches of the Yangtze River, a common trend was a clearly lower $PM_{2.5}$ value in 2014 than in 2013, but the general variation trend was not significant (Fig. 7c). A peak value of 33.7 $\mu g\,m^{-3}$ was observed in 2012 at Dongtan, followed by a decrease to 24.12 $\mu g\,m^{-3}$ over the subsequent two years. At Jinsha and Changde, the highest value was in 2013, while it was in 2009 at Lushan.

For the stations in southern China, a general decreasing trend was observed, with obvious fluctuations (Fig. 7d). Panyu is a typical station in the centre of the Pearl River Delta economic area of China. The $PM_{2.5}$ value decreased from 64.6 $\mu g\,m^{-3}$ in 2006 to 41.6 $\mu g\,m^{-3}$ in 2014, and the lowest value was 36.4 $\mu g\,m^{-3}$ in 2010. A similar trend was observed in Gulin, with a stronger fluctuation from 2010 to 2012. At Nanning, a peak value occurred in 2010 and the lowest value of 28.5 $\mu g\,m^{-3}$ was observed in 2012.

The general observations of the PM_{10} and PM_1 interannual variation trend were similar to the $PM_{2.5}$ at most stations. For example, a similar trend and fluctuations were observed at the stations presented in Figs. 8 and 7a. A difference in the trend was observed at Zhengzhou from 2013 to 2014, with a significant increasing trend of PM_{10} and decreasing trend of PM_1.

3.5 Diurnal variations

The average diurnal variations of $PM_{2.5}$ at various stations are presented in Fig. 9. Pronounced diurnal variations of $PM_{2.5}$ were observed in most urban sites with obvious morning peak around 7:00 to 8:00 a.m. and afternoon valley between 2:00 and 4:00 p.m. At some stations, evening peak can be recognized around 7:00 to 9:00 p.m. (Siping, Benxi, Fushun, Anshan, Guilin and Panyu) or midnight (Gucheng, Xian). This bimodal pattern was also observed in Beijing city (Zhao et al., 2009). The unimodal pattern without evening peak can be identified at some other stations (Zhengzhou, Shengyang and Nanning). In urban areas, the morning and evening peaks are contributed by enhanced anthropogenic activity during rush hour, and the afternoon valley is mainly due to higher atmospheric mixing layer which is benefit for air pollution diffusion. Panyu station is on top of a 140 m hill at the edge of Guangzhou city, so aged and mixing aerosols were observed with weakly urban diurnal variation pattern. Similar with Panyu station, the rural stations along the middle and lower reaches of the Yangtze River have no typical urban diurnal variation pattern (Fig. 9c).

3.6 Meteorological influences

Central-eastern China experienced severe haze events in January 2013 with regional stable planetary boundary layer and low mixing height (Wang et al., 2014). The daily averaged $PM_{2.5}$ concentrations and the meteorological factors of wind speed and relative humidity data in this period at Zhengzhou, Shenyang and Nanning were plotted in Fig. 10. Zhengzhou is located in this haze region with very high $PM_{2.5}$ concentrations especially from 6 to 15 January. The wind speed variation was negative related with $PM_{2.5}$ concentrations. The rapid increasing of $PM_{2.5}$ concentrations from 1 to 6 January was corresponding with the rapid decreasing of wind speed at same period. Also the big wind speed in 24 January resulted in low $PM_{2.5}$ concentration. Shenyang and Nanning are not located in this severe haze region, but still suffered some fine particle pollutant days in this month. The negative correlation between $PM_{2.5}$ and wind speed

ACPD
15, 15319–15354, 2015

were also observed at Shengyang and Nanning. In general, relative humidity (RH) variation was positive related with $PM_{2.5}$ concentrations if no precipitation occurred. Otherwise the high RH with precipitation correspondences low PM concentrations due to wet deposition.

For interannual variation, the negative correlation between $PM_{2.5}$ concentrations and wind speed and positive correlation between $PM_{2.5}$ concentrations and relative humidity cannot be well identified (Fig. 11). It reveals the emission variation possibly dominates the long-term PM concentration trend; meanwhile meteorological factors play a leading role during a short period.

4 Conclusions

Spatial and temporal trends in PM pollution were examined using PM_{10}, $PM_{2.5}$ and PM_1 concentration data at 24 stations from 2006 to 2014. Relatively high PM concentrations were observed at most stations. There were 14 stations that reached the PM_{10} annual air quality standard, but only 7 stations, mostly rural and remote stations, reached the $PM_{2.5}$ annual air quality standard of China. The highest PM concentrations were observed at the stations in the HBP and Guanzhong Plain. In addition, the percentage value of substandard days of $PM_{2.5}$ was greater than 50 %, indicating very serious air pollution in these regions. PM pollutants are also a serious problem in the industrial regions of northeast China and the Sichuan basin. The PM concentrations were relatively lower in the southern areas of China, but the averaged $PM_{2.5}$ concentration was still higher than the national standard.

As they are both fine particles, PM_1 and $PM_{2.5}$ were more correlated than $PM_{2.5}$ and PM_{10}. The correlations were sensitive to the effect of outlier data at those stations heavily impacted by dust storm events. More dust aerosol was observed in northern China, and thus the $PM_{2.5}/PM_{10}$ ratios increased from less than 0.6 to around 0.9 when moving from north to south China.

ACPD
15, 15319–15354, 2015

Pronounced seasonal variations were observed at most stations, with the highest concentrations in winter and lowest concentrations in summer. PM_{10} concentrations were also high in spring, due to the contribution of dust storm events, especially at those stations near to dust source regions. For $PM_{2.5}$ and PM_1, spring was a relatively low concentration season, especially at the stations in northern China. Also, low $PM_{2.5}/PM_{10}$ ratios were observed in spring in northern China.

An interannual decreasing trend was observed in the HBP and southern China from 2006 to 2014, but an increasing trend occurred at some stations in northeast China, and no significant trend could be found over the middle and lower reaches of the Yangtze River. Annual-averaged PM concentrations were lower in 2014 than 2013 at most stations, which may indicate an improvement in air quality following the "Action Plan for the Control of Air Pollution" document issued by the Chinese government in September 2013.

Bimodal and unimodal diurnal variation patterns were identified at urban stations. The negative correlation between PM concentrations and wind speed was found in a short period, but emission variation must to be considered for long-term trend analysis especially in rapid developing countries.

This network observation dataset provides the longest continuous record of fine particle concentrations in China, but it features a limited number of stations and an uneven spatial distribution. Importantly, there is no representative city site in the Yangtze River delta region, which is considered an important haze area in China. The emission sources and meteorological factors influencing PM spatial and temporal patterns in China still require further study.

Acknowledgements. This work was supported by grants from the National Key Project of Basic Research (2014CB441201), the National Natural Science Foundation of China (41275167) and the Chinese Academy of Meteorological Sciences (2013Z007). It was also supported by the Climate Change Collaborative Innovation Center and the CMA Innovation Team of Haze-fog Observation and Forecasts.

References

Brook, J. R., Dann, T. F., and Burnett, R. T.: The relationship among TSP, PM_{10}, $PM_{2.5}$, and Inorganic constituents of atmospheric particulate matter at multiple Canadian locations, J. Air Waste Manage. Assoc., 47, 2–19, 1997.

Cao, J.-J., Shen, Z.-X., Chow, J. C., Watson, J. G., Lee, S.-C., Tie, X.-X., Ho, K.-F., Wang, G.-H., and Han, Y.-M.: Winter and summer $PM_{2.5}$ chemical compositions in fourteen Chinese cities, J. Air Waste Manage., 62, 1214–1226, 2012.

Chen, S., Huang, J., Zhao, C., Qian, Y., Leung, R., and Yang, B.: Modeling the transport and radiative forcing of Taklimakan dust over the Tibetan Plateau: a case study in the summer of 2006, J. Geophys. Res., 118, 797–812, 2013.

Delfino, R. J., Sioutas, C., and Malik, S.: Potential role of ultrafine particles in associations between airborne particle mass and cardiovascular health, Environ. Health Persp., 113, 934–946, 2005.

Eldred, R. A., Cahill, T. A., and Flocchini, R. G.: Composition of $PM_{2.5}$ and PM_{10} aerosols in the IMPROVE network, J. Air Waste Manage., 47, 194–203, 1997.

Gehrig, R. and Buchmann, B.: Characterising seasonal variations and spatial distribution of ambient PM_{10} and $PM_{2.5}$ concentrations based on long-term Swiss monitoring data, Atmos. Environ., 37, 2571–2580, 2003.

Gomiscek, B., Hauck, H., Stopper, S., and Preining, O.: Spatial and temporal variations of PM_1, $PM_{2.5}$, PM_{10} and particle number concentration during the AUPHEP – project, Atmos. Environ., 38, 3917–3934, 2004.

Grimm, H. and Eatough, D. J.: Aerosol measurement: the use of optical light scattering for the determination of particulate size distribution, and particulate mass, including the semi-volatile fraction, J. Air Waste Manage., 59, 101–107, 2009.

Hansen, J. C., Woolwine III, W. R., Bates, B. L., Clark, J. M., Kuprov, R. Y., Mukherjee, P., Murray, J. A., Simmons, M. A., Waite, M. F., Eatough, N. L., Eatough, D. J., Long, R., and Grover, B. D.: Semicontinuous $PM_{2.5}$ and PM_{10} mass and composition measurements in Lindon, Utah, during winter 2007, J. Air Waste Manage., 60, 346–355, 2010.

Haywood, J. and Boucher, O.: Estimates of the direct and indirect radiative forcing due to tropospheric aerosols: a review, Rev. Geophys., 38, 513–543, 2000.

He, K., Yang, F., Ma, Y., Zhang, Q., Yao, X., Chan, C. K., Cadle, S., Chan, T., and Mulawa, P.: The characteristics of $PM_{2.5}$ in Beijing, China, Atmos. Environ., 35, 4959–4970, 2001.

ACPD
15, 15319–15354, 2015

Houthuijs, D., Breugelmans, O., Hoek, G., Vaskövi, É., Miháliková, E., Pastuszka, J. S., Jirik, V., Sachelarescu, S., Lolova, D., Meliefste, K., Uzunova, E., Marinescu, C., Volf, J., Leeuw, F. D., van de Wiel, H., Fletcher, T., Lebret, E., and Brunekreef, B.: PM_{10} and $PM_{2.5}$ concentrations in Central and Eastern Europe: results from the Cesar study, Atmos. Environ., 35, 2757–2771, 2001.
Li, C., Mao, J., Lau, K.-H. A., Chen, J.-C., Yuan, Z., Liu, X., Zhu, A., and Liu, G.: Characteristics of distribution and seasonal variation of aerosol optical depth in eastern China with MODIS products, Chinese Sci. Bull., 48, 2488–2495, 2003.
Luo, Y., Lu, D., Zhou, X., Li, W., and He, Q.: Characteristics of the spatial distribution and yearly variation of aerosol optical depth over China in last 30 years, J. Geophys. Res., 106, 14501–14513, 2001.
Malm, W. C., Schichtel, B. A., Pitchford, M. L., Ashbaugh, L. L., and Eldred, R. A.: Spatial and monthly trends in speciated fine particle concentration in the United States, J. Geophys. Res., 109, D03306, doi:10.1029/2003JD003739, 2004.
Oberdörster, G., Oberdörster, E., and Oberdörster, J.: Nanotoxicology: an emerging discipline evolving from studies of ultrafine particles, Environ. Health Persp., 113, 823–839, 2005.
Pope III, C. A. and Dockery, D. W.: Health effects of fine particulate air pollution: lines that connect, J. Air Waste Manage., 56, 709–742, 2006.
Qian, W. H., Tang, X., and Quan, L. S.: Regional characteristics of dust storms in China, Atmos. Environ., 38, 4895–4907, 2004.
Qu, W.-J., Zhang, X.-Y., Arimoto, R., Wang, Y.-Q., Wang, D., Sheng, L.-F., and Fu, G.: Aerosol background at two remote CAWNET sites in western China, Sci. Total Environ., 407, 3518–3529, 2009.
Qu, W.-J., Arimoto, R., Zhang, X. Y., Zhao, C. H., Wang, Y. Q., Sheng, L. F., and Fu, G.: Spatial distribution and interannual variation of surface PM_{10} concentrations over eighty-six Chinese cities, Atmos. Chem. Phys., 10, 5641–5662, doi:10.5194/acp-10-5641-2010, 2010.
Ramanathan, V., Crutzen, P. J., Kiehl, J. T., and Rosenfeld, D.: Aerosols, climate, and the hydrological cycle, Science, 294, 2119–2124, 2001.
Tiwari, S., Chate, D. M., Pragya, P., Ali, K., and Bisht, D. S.: Variations in mass of the PM_{10}, $PM_{2.5}$ and PM_1 during the monsoon and winter at New Delhi, Aerosol Air Qual. Res., 12, 20–29, 2012.

ACPD
15, 15319–15354, 2015

Wang, G., Huang, L., Gao, S., Gao, S., and Wang, L.: Measurements of PM_{10} and $PM_{2.5}$ in urban area of Nanjing, China and the assessment of pulmonary deposition of particle mass, Atmos. Environ., 48, 689–695, 2002.

Wang, H., Xu, J., Zhang, M., Yang, Y., Shen, X., Wang, Y., Chen, D., and Guo, J.: A study of the meteorological causes of a prolonged and severe haze episode in January 2013 over central-eastern China, Atmos. Environ., 98, 146–157, 2014.

Wang, X., Bi, X., Sheng, G., and Fu, J.: Chemical composition and sources of PM_{10} and $PM_{2.5}$ aerosols in Guangzhou, China, Environ. Monit. Assess., 119, 425–439, 2006.

Wang, Y. Q., Zhang, X. Y., Gong, S. L., Zhou, C. H., Hu, X. Q., Liu, H. L., Niu, T., and Yang, Y. Q.: Surface observation of sand and dust storm in East Asia and its application in CUACE/Dust, Atmos. Chem. Phys., 8, 545–553, doi:10.5194/acp-8-545-2008, 2008.

Watson, J.: Visibility: science and regulation, J. Air Waste Manage., 52, 628–713, 2002.

Wei, F., Teng, E., Wu, G., Hu, W., Wilson, W. E., Chapman, R. S., Pau, J. C., and Zhang, J.: Ambient concentrations and elemental composition of PM_{10} and $PM_{2.5}$ in four Chinese cities, Environ. Sci. Technol., 33, 4188–4193, 1999.

Yao, X., Chan, C. K., Fang, M., Cadle, S., Chan, T., Mulawa, P., He, K., and Ye, B.: The water-soluble ionic composition of $PM_{2.5}$ in Shanghai and Beijing, China, Atmos. Environ., 36, 4223–4234, 2002.

Zhang, Q., Streets, D. G., Carmichael, G. R., He, K. B., Huo, H., Kannari, A., Klimont, Z., Park, I. S., Reddy, S., Fu, J. S., Chen, D., Duan, L., Lei, Y., Wang, L. T., and Yao, Z. L.: Asian emissions in 2006 for the NASA INTEX-B mission, Atmos. Chem. Phys., 9, 5131–5153, doi:10.5194/acp-9-5131-2009, 2009.

Zhang, X. Y., Gong, S. L., Zhao, T. L., Arimoto, R., Wang, Y. Q., and Zhou, Z. J.: Sources of Asian dust and role of climate change versus desertification in Asian dust emission, Geophys. Res. Lett., 30, 2272 doi:10.1029/2003GL018206, 2003.

Zhang, X. Y., Wang, Y. Q., Niu, T., Zhang, X. C., Gong, S. L., Zhang, Y. M., and Sun, J. Y.: Atmospheric aerosol compositions in China: spatial/temporal variability, chemical signature, regional haze distribution and comparisons with global aerosols, Atmos. Chem. Phys., 12, 779–799, doi:10.5194/acp-12-779-2012, 2012.

Zhao, X., Zhang, X., Xu, X., Xu, J., Meng, W., and Pu, W.: Seasonal and diurnal variations of ambient $PM_{2.5}$ concentration in urban and rural environments in Beijing, Atmos. Environ., 43, 2893–2900, 2009.

ACPD
15, 15319–15354, 2015

Zheng, M., Salmon, L. G., Schauer, J. J., Zeng, L., Kiang, C. S., Zhang, Y., and Cass, G. R.: Seasonal trends in $PM_{2.5}$ source contributions in Beijing, China, Atmos. Environ., 39, 3967–3976, 2005.
Zhou, Z. J. and Zhang, G. C.: Typical severe dust storms in northern China during 1954–2002, Chinese Sci. Bull., 48, 2366–2370, 2003.

Discussion Paper | Discussion Paper | Discussion Paper | Discussion Paper |

ACPD
15, 15319–15354, 2015

Spatial and temporal variations of the concentrations of PM_{10}, $PM_{2.5}$ and PM_1 in China

Y. Q. Wang et al.

Table 1. Description of the PM stations.

Stations	Latitude (° N)	Longitude (° E)	Altitude (m)	Start Time	Description
Zhengzhou	34.78	113.68	99.0	1/2006	Urban, in the center of Zhengzhou city, 56 m building.
Chengdu	30.65	104.04	496.0	3/2006	Urban, in the center of Chengdu city, 91 m building.
Xian	34.43	108.97	363.0	1/2006	Urban, in northern margin of Xian city, 20 km north of center of Xian city, 4 m sampling container.
Nanning	22.82	108.35	84.0	1/2006	Urban, in Nanning city, 140 m hill.
Anshan	41.05	123.00	78.3	10/2007	Urban, in Anshan city, 10 m building.
Shenyang	41.76	123.41	110.0	10/2007	Urban, in Shenyang city, 15 m building.
Benxi	41.19	123.47	185.4	10/2007	Urban, in Benxi city, 12 m building.
Fushun	41.88	123.95	163.0	10/2007	Urban, in Fushun city, 10 m building.
Qingdao	36.07	120.33	77.2	3/2007	Urban, in Qingdao city, top of Fulongshan hill.
Lhasa	29.67	91.13	3663.0	1/2006	Urban, in Lhasa city, 7 m building.
Siping	43.18	124.33	165.4	3/2007	Urban, in Siping city, 4 m sampling container.
Panyu	23.00	113.35	5.0	1/2006	Suburban, in Panyu district of Guangzhou city, 140 m hill.
Gucheng	39.13	115.80	15.2	1/2006	Suburban, 38 km southwest of Baoding city, within area of rapid urbanization, 8 m building.
Chifeng	42.27	118.97	568.0	3/2007	Rural, suburbs of Chifeng city, 4 m sampling container.
Dandong	40.05	124.33	13.9	3/2007	Rural, suburbs of Dandong city, 4 m sampling container.
Erlianhaote	43.65	111.97	965.9	3/2007	Rural, suburbs of Erlianhaote city, 4 m sampling container.
Yulin	38.43	109.20	1135.0	1/2006	Rural, 10 km north of Yulin city, at the southeastern edge of Mu Us desert.
Jinsha	29.63	114.20	416.0	4/2006	Rural, 105 km north of Wuhan city, 8 m building.
Guilin	25.32	110.30	164.4	1/2006	Rural, north margin of Guilin city, meteorological observation field.
Lushan	29.57	115.99	1165.0	1/2006	Rural, Kuniubei peak of Mount Lu.
Changde	29.17	111.71	563.0	1/2006	Rural, 18 km northwest from Changde city, 8 m building.
Dongtan	31.50	121.80	10.0	5/2009	Rural, east of Chongming island near Shanghai.
Akdala	47.12	87.97	562.0	9/2006	Remote, 55 km west of Fuhai county, 10 m building.
Shangri-La	28.02	99.73	3580.0	10/2006	Remote, 12 km northeast of Shangri-La county.

ACPD
15, 15319–15354, 2015

Table 2. Averaged PM_{10}, $PM_{2.5}$ and PM_1 concentrations and their interrelationships at each station.

Stations	Averaged PM concentrations ($\mu g\ m^{-3}$)[a]			SB ratio (PM_{10})[b]	SB ratio ($PM_{2.5}$)[b]	$PM_{2.5}/PM_{10}$	$PM_1/PM_{2.5}$	R^2 ($PM_{2.5}$ to PM_{10})	R^2 (PM_1 to $PM_{2.5}$)
	PM_{10}	$PM_{2.5}$	PM_1						
Zhengzhou	131.7 (84.4)	84.8 (47.4)	71.0 (40.5)	0.31	0.51	0.68	0.84	0.68	0.91
Chengdu	78.0 (72.5)	59.5 (42.2)	52.7 (35.4)	0.11	0.27	0.83	0.91	0.76	0.94
Xian	135.4 (97.3)	93.6 (67.3)	77.0 (55.6)	0.34	0.52	0.73	0.83	0.77	0.93
Nanning	51.2 (56.3)	38.4 (24.7)	34.9 (22.2)	0.01	0.08	0.77	0.91	0.52	0.97
Anshan	97.8 (62.9)	60.9 (42.9)	52.3 (39.0)	0.17	0.25	0.65	0.85	0.72	0.98
Shenyang	85.0 (58.2)	59.1 (42.7)	50.8 (36.7)	0.11	0.25	0.69	0.85	0.88	0.97
Benxi	97.6 (57.4)	66.7 (45.0)	54.8 (36.4)	0.13	0.30	0.69	0.82	0.81	0.94
Fushun	80.3 (54.2)	50.1 (31.7)	42.8 (28.3)	0.07	0.17	0.66	0.85	0.64	0.97
Qingdao	64.8 (52.1)	47.3 (34.0)	41.1 (30.5)	0.05	0.17	0.76	0.86	0.76	0.95
Lhasa	37.7 (30.8)	14.0 (10.7)	9.6 (8.6)	0.01	0.00	0.40	0.66	0.72	0.94
Panyu	58.7 (33.1)	44.5 (24.4)	39.7 (22.1)	0.02	0.12	0.77	0.89	0.95	0.98
Gucheng	127.8 (75.1)	89.7 (53.0)	79.4 (48.8)	0.31	0.54	0.71	0.87	0.79	0.97
Siping	83.3 (54.3)	55.4 (35.2)	48.5 (32.5)	0.10	0.22	0.68	0.86	0.71	0.96
Chifeng	88.0 (68.9)	42.4 (33.1)	32.6 (27.8)	0.17	0.14	0.51	0.75	0.72	0.92
Dandong	66.8 (44.0)	45.6 (24.8)	39.3 (21.3)	0.03	0.11	0.71	0.86	0.64	0.90
Erlianhaote	49.1 (80.2)	22.0 (22.6)	15.9 (14.7)	0.03	0.03	0.51	0.72	0.71	0.61
Yulin	66.6 (67.1)	31.2 (21.0)	22.4 (15.9)	0.06	0.03	0.54	0.72	0.54	0.61
Jinsha	42.0 (38.6)	33.6 (24.1)	30.5 (21.9)	0.01	0.06	0.85	0.90	0.63	0.89
GuiLin	57.6 (50.5)	46.5 (30.8)	41.7 (27.1)	0.04	0.15	0.85	0.90	0.70	0.96
Lushan	45.4 (32.7)	37.8 (27.9)	33.2 (26.7)	0.01	0.09	0.85	0.86	0.91	0.95
Changde	45.7 (33.8)	40.3 (29.1)	37.0 (27.5)	0.01	0.12	0.89	0.91	0.93	0.96
Dongtan	31.9 (34.0)	27.4 (25.9)	24.8 (23.8)	0.01	0.06	0.90	0.90	0.92	0.96
Akdala	17.1 (57.6)	9.8 (13.7)	7.7 (6.9)	0.00	0.00	0.67	0.79	0.80	0.53
Shangri-La	6.8 (6.3)	5.2 (5.3)	4.5 (5.0)	0.00	0.00	0.76	0.81	0.94	0.99

[a] Arithmetic mean value with standard deviation in parentheses.
[b] The ratio of substandard days (daily averaged PM_{10} or $PM_{2.5}$ concentrations that exceed the standard values) to total observation days.

ACPD
15, 15319–15354, 2015

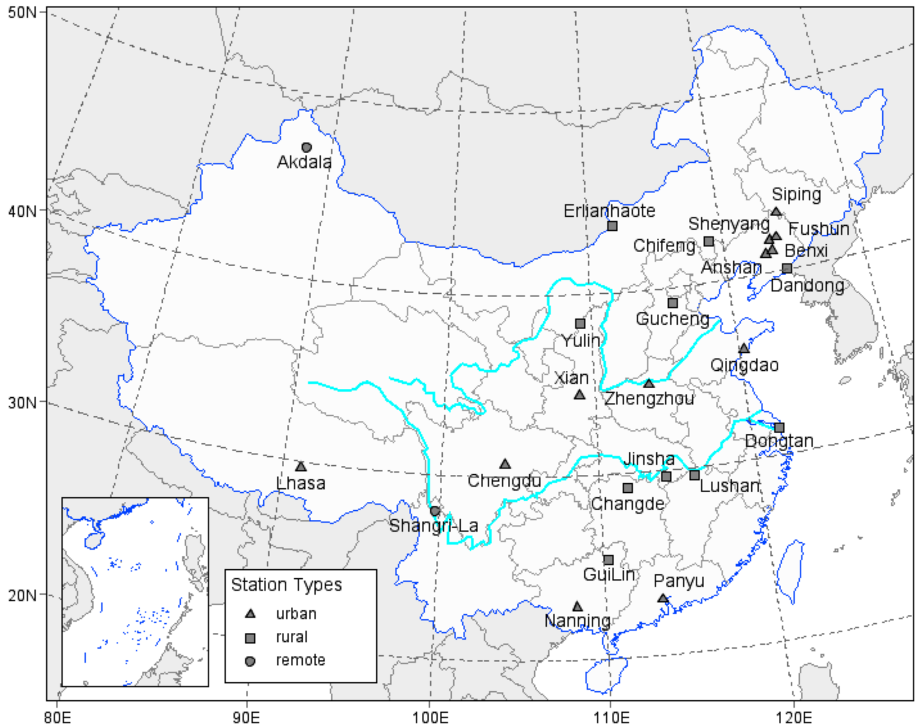

Figure 1. Distribution of the PM observation stations used in this study.

ACPD
15, 15319–15354, 2015

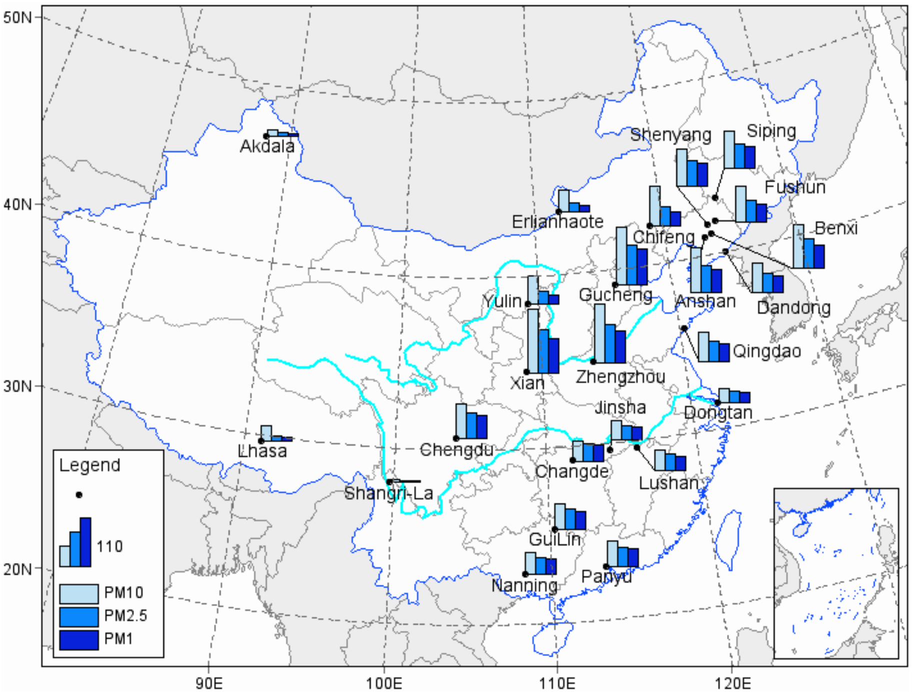

Figure 2. Map showing bar charts of average PM_{10}, $PM_{2.5}$ and PM_1 concentration ($\mu g\,m^{-3}$) distributions at the observation stations.

ACPD
15, 15319–15354, 2015

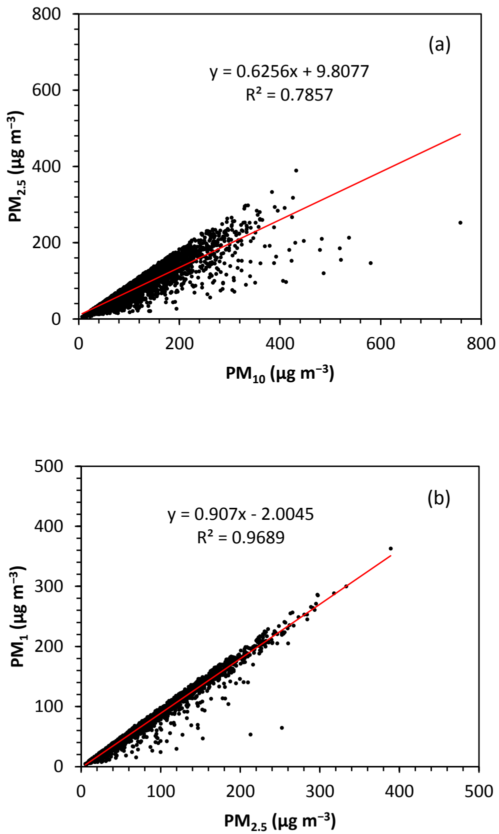

Figure 3. Scatterplots of **(a)** $PM_{2.5}$ vs. PM_{10} and **(b)** PM_1 vs. $PM_{2.5}$ at Gucheng.

ACPD
15, 15319–15354, 2015

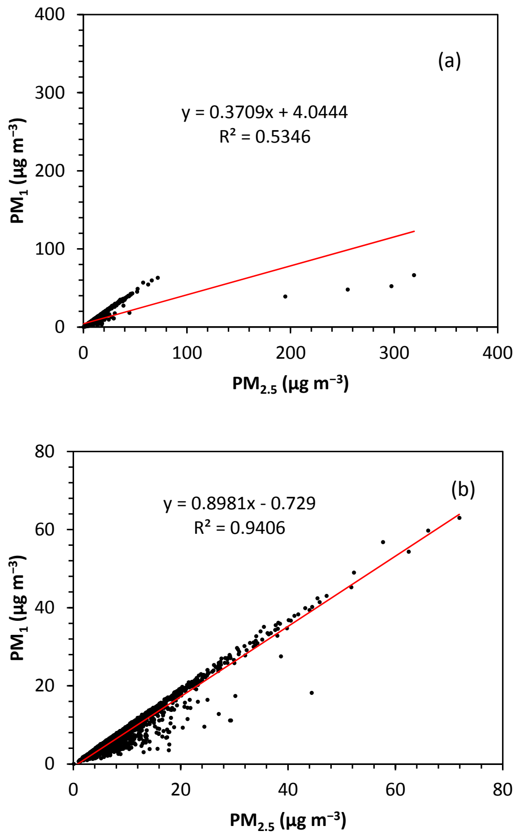

Figure 4. Scatterplots of PM_1 vs. $PM_{2.5}$ **(a)** with and **(b)** without data from the strong sand and dust storm at Akdala.

ACPD
15, 15319–15354, 2015

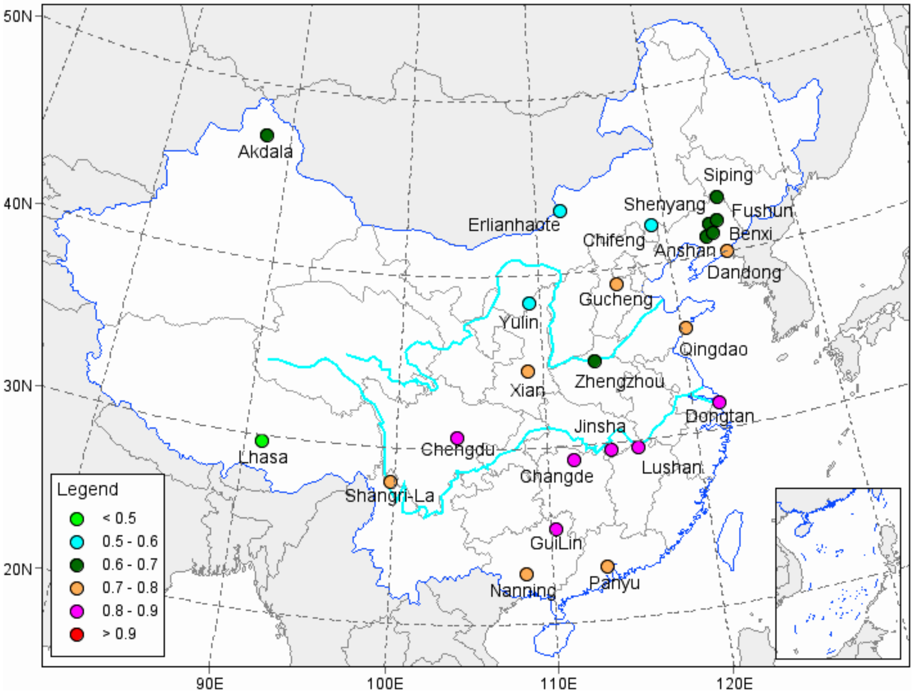

Figure 5. Spatial distribution of the average ratios of $PM_{2.5}/PM_{10}$.

ACPD
15, 15319–15354, 2015

Spatial and temporal variations of the concentrations of PM_{10}, $PM_{2.5}$ and PM_1 in China

Y. Q. Wang et al.

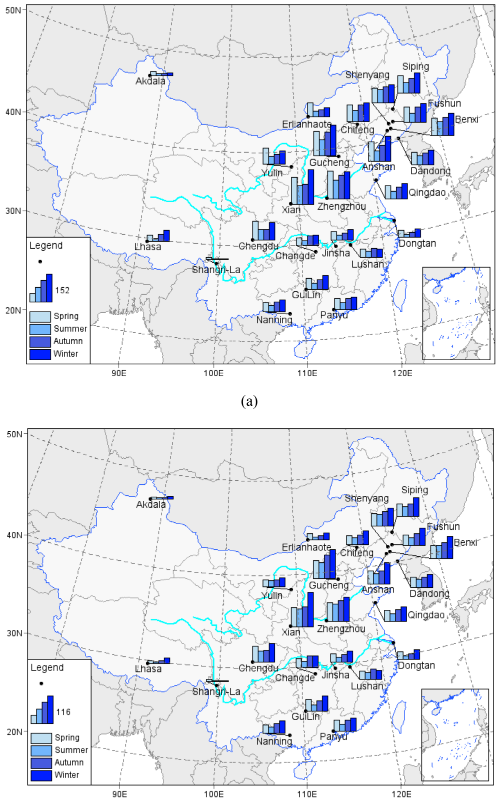

Figure 6.

ACPD

15, 15319–15354, 2015

Spatial and temporal variations of the concentrations of PM_{10}, $PM_{2.5}$ and PM_1 in China

Y. Q. Wang et al.

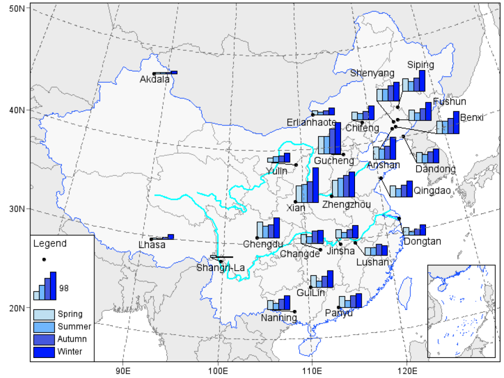

(c)

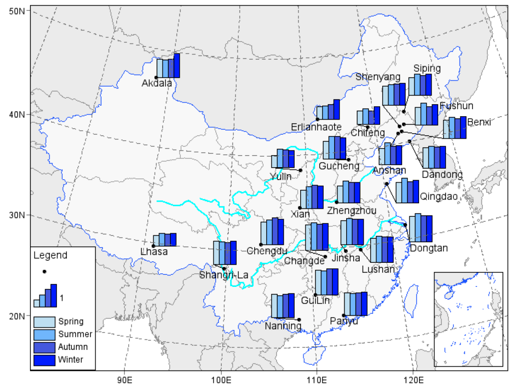

(d)

Figure 6. Spatial distribution of the seasonal average concentrations (µg m^{-3}) of **(a)** PM_{10}, **(b)** $PM_{2.5}$, **(c)** PM_1 and **(d)** ratios of $PM_{2.5}/PM_{10}$.

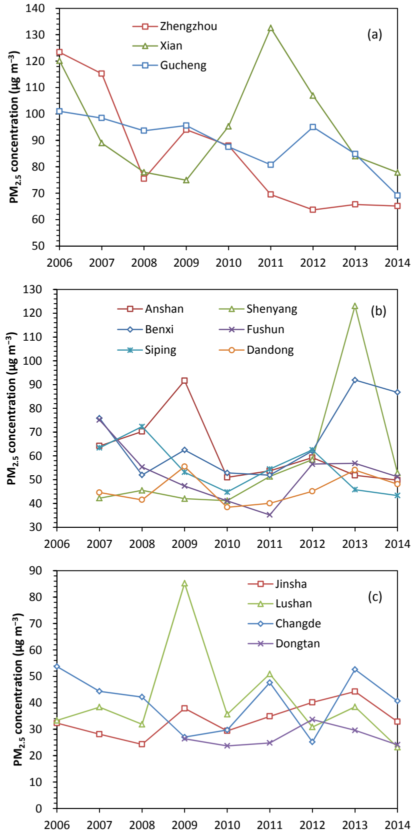

Figure 7.

ACPD

15, 15319–15354, 2015

Spatial and temporal variations of the concentrations of PM_{10}, $PM_{2.5}$ and PM_1 in China

Y. Q. Wang et al.

Title Page
Abstract Introduction
Conclusions References
Tables Figures
Back Close
Full Screen / Esc
Printer-friendly Version
Interactive Discussion

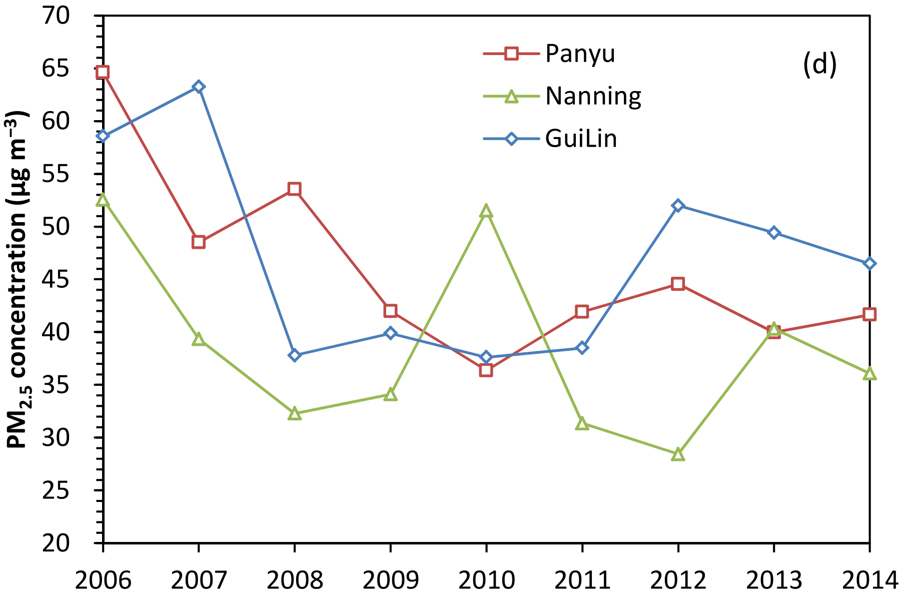

Figure 7. Interannual variations of $PM_{2.5}$ concentrations at **(a)** the stations in the HBP and Guanzhong Plain, **(b)** the stations in northeast China, **(c)** the stations along the middle and lower reaches of the Yangtze River, and **(d)** the stations in southern China.

ACPD
15, 15319–15354, 2015

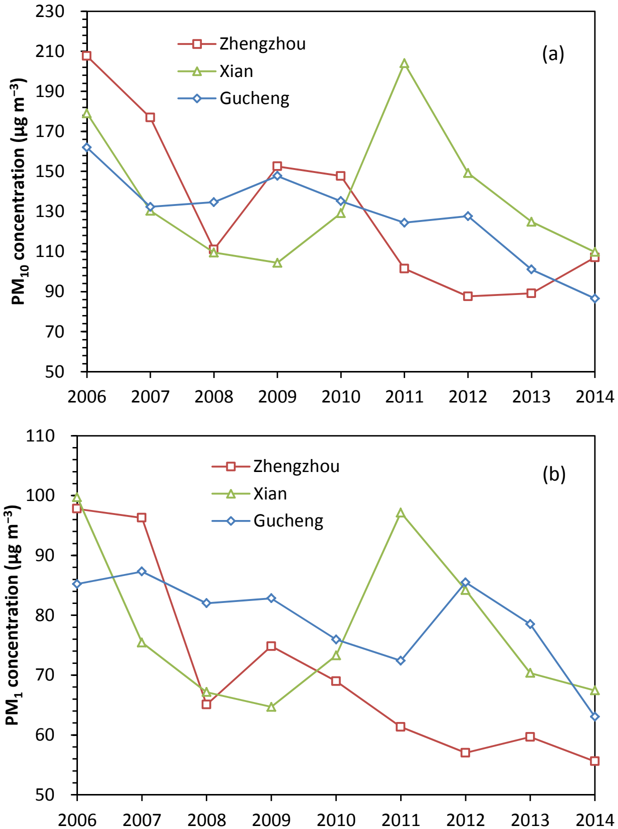

Figure 8. Interannual variations of **(a)** PM_{10} concentrations and **(b)** PM_1 concentrations at Zhengzhou, Xian and Gucheng.

ACPD
15, 15319–15354, 2015

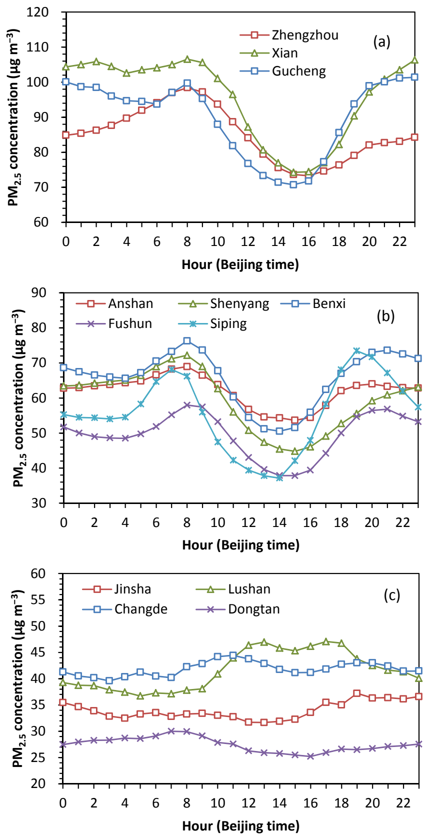
PM2.5 concentration (μg m−3)
Zhengzhou
Xian
Gucheng
(a)
Hour (Beijing time)
Anshan
Shenyang
Benxi
Fushun
Siping
(b)
Jinsha
Lushan
Changde
Dongtan
(c)

Figure 9.

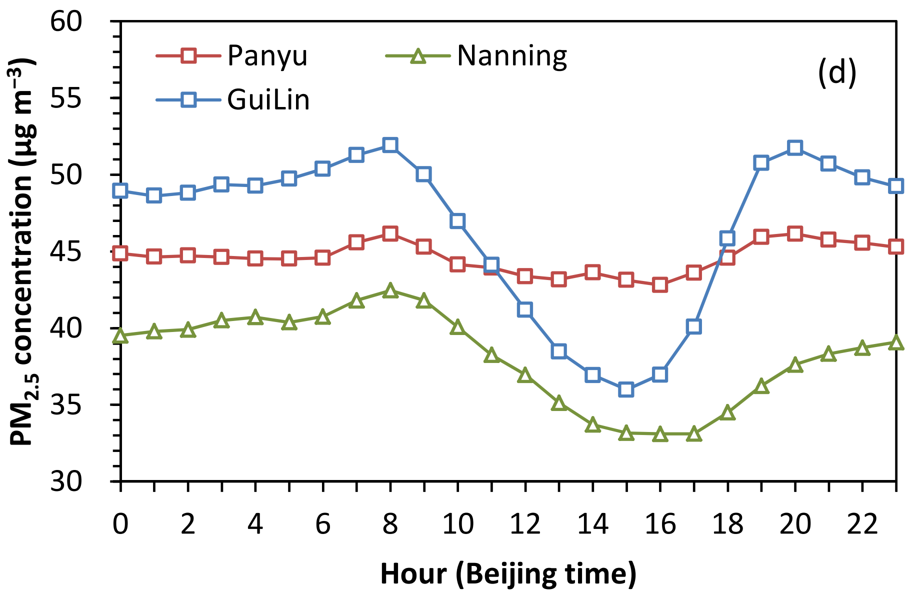

Figure 9. Diurnal variations of $PM_{2.5}$ concentrations at **(a)** the stations in the HBP and Guanzhong Plain, **(b)** the stations in northeast China, **(c)** the stations along the middle and lower reaches of the Yangtze River, and **(d)** the stations in southern China.

ACPD
15, 15319–15354, 2015

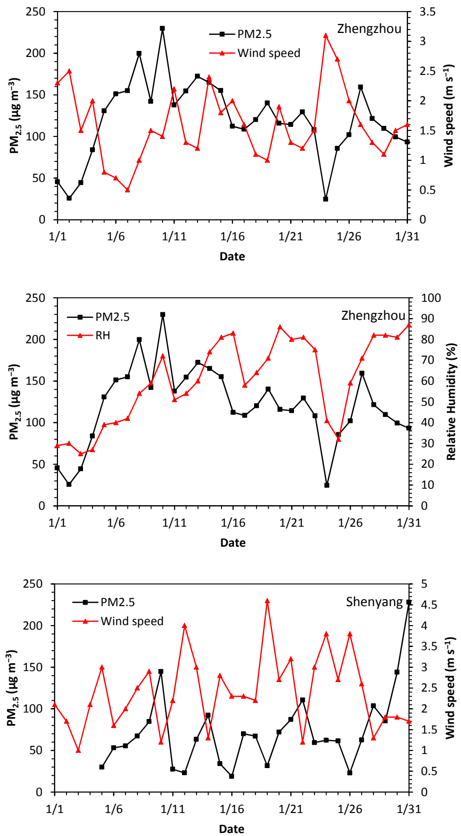

Figure 10.

ACPD
15, 15319–15354, 2015

Spatial and temporal variations of the concentrations of PM_{10}, $PM_{2.5}$ and PM_1 in China

Y. Q. Wang et al.

Title Page
Abstract Introduction
Conclusions References
Tables Figures
Back Close
Full Screen / Esc
Printer-friendly Version
Interactive Discussion

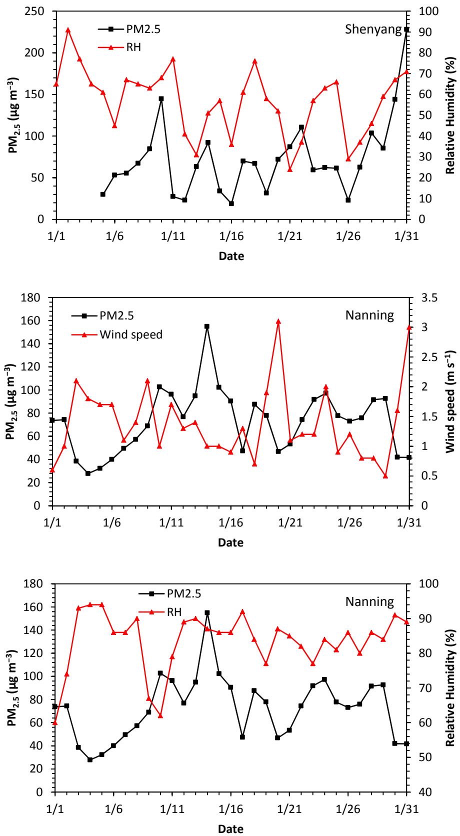

Figure 10. Daily averaged $PM_{2.5}$ concentrations vs. wind speed and relative humidity data at Zhengzhou, Shenyang and Nanning in January 2013.

ACPD
15, 15319–15354, 2015

Spatial and temporal variations of the concentrations of PM_{10}, $PM_{2.5}$ and PM_1 in China

Y. Q. Wang et al.

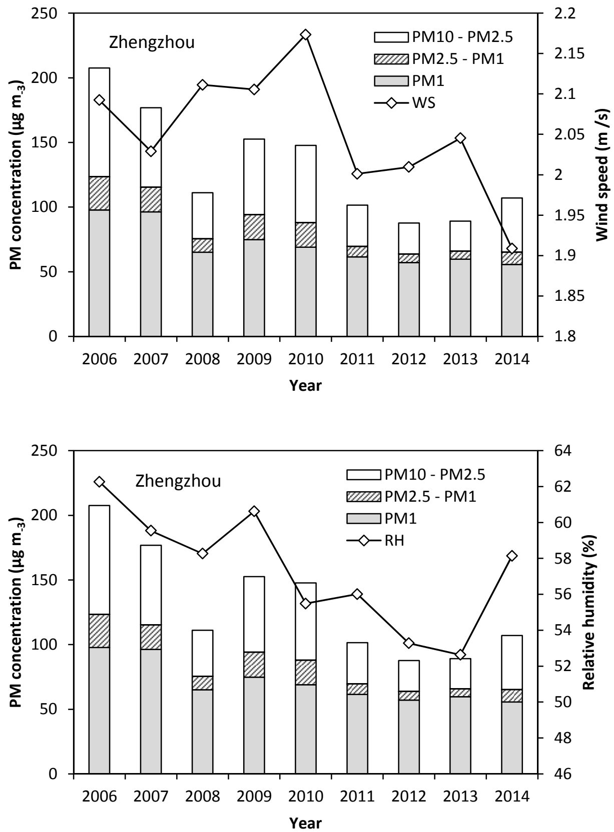

Figure 11.

ACPD

15, 15319–15354, 2015

Spatial and temporal variations of the concentrations of PM_{10}, $PM_{2.5}$ and PM_1 in China

Y. Q. Wang et al.

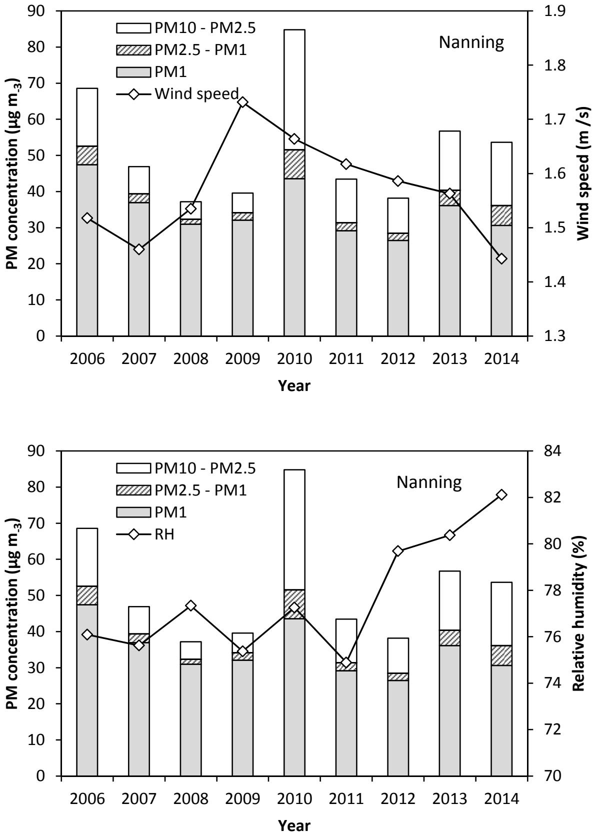

Figure 11. Interannual variations of PM_{10}, $PM_{2.5}$ and PM_1 vs. wind speed and relative humidity at Zhengzhou and Nanning.

ACPD
15, 15319–15354, 2015

Spatial and temporal variations of the concentrations of PM_{10}, $PM_{2.5}$ and PM_1 in China

Y. Q. Wang et al.

Title Page
Abstract Introduction
Conclusions References
Tables Figures
Back Close
Full Screen / Esc
Printer-friendly Version
Interactive Discussion